

Seismic response control of a building complex utilizing passive friction damper: Analytical study

C. L. Ng[†] and Y. L. Xu[‡]

*Department of Civil and Structural Engineering, The Hong Kong Polytechnic University,
Hung Hom, Kowloon, Hong Kong, China*

(Received April 20, 2005, Accepted September 9, 2005)

Abstract. Control of structural response due to seismic excitation in a manner of coupling adjacent buildings has been actively developed, and most attention focused on those buildings of similar height. However, with the rapid development of some modern cities, multi-story buildings constructed with an auxiliary low-rise podium structure to provide extra functions to the complex become a growing construction scheme. Being inspired by the positively examined coupling control approach for buildings with similar height, this paper aims to provide a comprehensive analytical study on control effectiveness of using friction dampers to link the two buildings with significant height difference to supplement the recent experimental investigation carried out by the writers. The analytical model of a coupled building system is first developed with passive friction dampers being modeled as Coulomb friction. To highlight potential advantage of coupling the main building and podium structure with control devices that provide a lower degree of coupling, the inherent demerit of rigid-coupled configuration is then evaluated. Extensive parametric studies are finally performed. The concerned parameters influencing the design of optimal friction force and control efficiency include variety of earthquake excitation and differences in floor mass, story number as well as number of dampers installed between the two buildings. In general, the feasibility of interaction control approach applied to the complex structure for vibration reduction due to seismic excitation is supported by positive results.

Key words: coupling control; analytical study; passive friction damper; Coulomb friction; seismic excitation.

1. Introduction

Associated with the economic development of modern cities, more building structures appear with stylistic shape or extraordinary height as a landmark and prosperous indication of the cities. Main buildings with medium- to high-rise level constructed with an auxiliary podium structure, based upon both functional and architectural considerations, are one of the growing construction schemes. However, it is intuitive that this complex structure is in a form of setback building because both structures are very likely integrated with rigid elements in most civil engineering practice. For such types of structures with vertical irregular configuration, serious torsional effect and concentration of inelastic action at the level of setback were observed during some past earthquakes and resulted in

[†] Ph.D. Candidate

[‡] Professor, Corresponding author, E-mail: ceylxu@polyu.edu.hk

poor performance of the structures (Suzuki 1971, Gardis *et al.* 1982, Arnold 1980, Arnold and Elsesser 1980).

To avoid or limit excessive inelastic deformation experienced by structural elements leading to permanent damage during seismic attacks, addition of energy damping systems in the structure to dissipate much of earthquake-induced energy is undoubtedly a sensible choice. Their efficacy to enhance energy absorbing capacity of the buildings is extensively supported by the state-of-the-art publications (Hanson *et al.* 1993, Soong and Dargush 1997, Constantinou *et al.* 1998). In most of these applications, damping devices assembled with diagonal or chevron bracing components are often a well-accepted practice. It is, however, generally recognized that ineffective energy dissipation under such configuration might be resulted in a stiff structural system, which is probably the case of podium structure, because of relatively small drifts and interstory velocities. One solution is to increase the size or number of damping devices, while obstructions in open frames are inevitably caused which is definitely not preferable from the view point of owner. Other schemes, of which the ordinary bracing is replaced by an amplifying bracing system to magnify the limited drifts and interstory velocities, were also proposed to address this problem (Taylor 2002, Constantinou *et al.* 2001, Gluck and Ribakov 2001, Ribakov and Reinhorn 2003).

Despite energy dissipation ability is effectively restored or improved by the modified arrangement of damper-brace assembly, it may sound attractive if the supplemental damping devices could be mounted outside the buildings to maximize the internal space for architectural use, while still absorbing unwanted energy from structures. In this connection, the coupling control method was suggested to apply in the building complex. This novel control scenario was first proposed by Klein *et al.* (1972), which the essence is to attenuate vibration responses of dissimilar adjacent structures by imparting forces to one another with the aid of interconnected control devices. Afterwards, attention was gradually received and numerous studies on interaction control of adjacent structures with passive-natured supplemental damping devices were undertaken aiming to address various engineering problems. Westermo (1989) studied the feasibility of connecting closely neighboring buildings using hinged links for the purpose of preventing pounding during earthquakes. Gurley *et al.* (1994) intended to enhance wind-resistance of high-rise buildings by jointing them together with a single force link. To overcome the insufficient countervailing force generated by tuned mass dampers (TMDs) or too large energy requirement for active mass drivers (AMDs) employed in flexible high-rise buildings, Kamagata *et al.* (1996) suggested using the coupled building control method with passive devices of which optimal stiffness and damping are designed according to LQ control theory and suboptimal control theory. Other methods, the extended theory of stationary points P & Q and the genetic algorithms, to determine the optimal parameters of joint dampers were also adopted by Kageyama *et al.* (1999) and Sugino *et al.* (1999), respectively.

Although aforementioned studies revealed that the seismic resistance of coupled buildings with similar height was strengthened, whether competent performance could be obtained in coupled structures, which considerably differ in height, is questionable. Thus, the extension of coupling control technique to the building complex with significant height difference has been experimentally investigated by the writers recently through shaking table tests (Ng and Xu 2004). Two elastic shear building models in 12- and 3-story were used as mock-up of a multi-story main building and a podium structure, respectively. In the experiment, the building models in uncoupled, rigid-coupled and passive friction damper-coupled configurations were all studied. In spite of the preliminary experimental investigation reported with positive results, the considered models were in small scale and represented a specific coupled system. The achievement of control performance for variety of

building configurations and the effects of damper parameters on the control performance have not yet been studied thoroughly. To this end, a systematic analytical study is conducted in this paper to supplement the knowledge in this subject. The analytical study starts with establishing an analytical model of coupled building systems. Dynamic implications of the main building in rigid connection to the podium structure are subsequently investigated by means of reformulated modal analysis method to explore the reason of unfavorable dynamic response enlargement. Extensive parametric studies are performed to illustrate the optimal design of friction force, as well as to characterize the effects on control effectiveness with respect to the building height, floor masses and input of earthquakes.

2. Modeling of coupled building systems

2.1 Governing equation of motion

Fig. 1 illustrates a coupled building system consisting of two dissimilar buildings, main building (building 1) and podium structure (building 2), of N_1 and N_2 ($N_1 \geq N_2$) stories, respectively, connected by N passive friction dampers ($N \leq N_2 \leq N_1$) at some stories. Each building is ideally

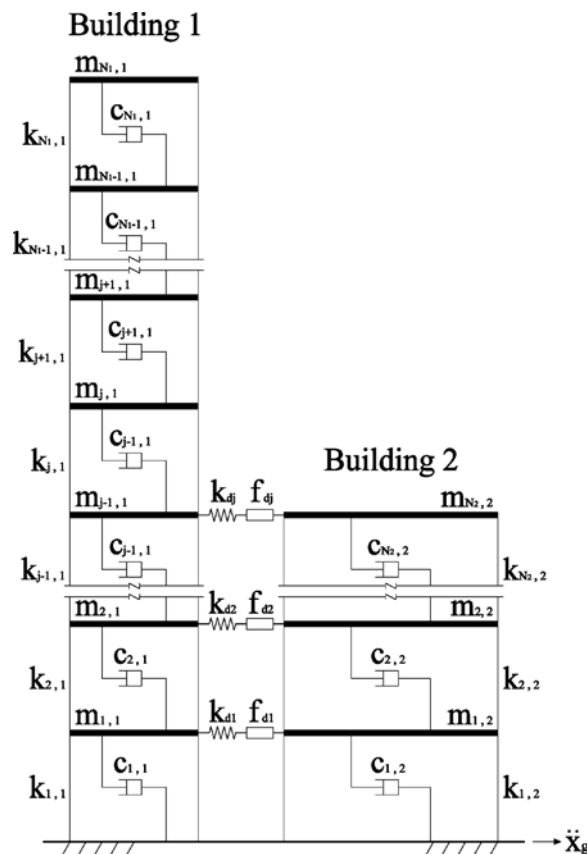


Fig. 1 Schematic diagram of coupled building system

modeled as a linear elastic shear building with one translational degree of freedom for each floor. The mass of each building is concentrated at its rigid floor diaphragms and the shear stiffness is provided by its column. Idealization on the same floor elevation for the buildings is considered. The friction dampers interconnecting the structures at the floors are modeled as an assembly of an elastic connector and a friction slider connected in series. It is further specified that both buildings are subjected to the same base acceleration and any effects due to spatial variations of the ground motion or due to the soil-structure interactions are neglected. Such assumption on negligible spatial variations of ground motion is justified from the fact that, in most cases, both structures are deemed to be built on a common raft or a rigid cap foundation.

The equation of motion of the coupled building system, in terms of the relative displacement vector $\mathbf{x}(t) = [\mathbf{x}_1^T(t) \ \mathbf{x}_2^T(t)]^T$ with respect to its base, is written by

$$\mathbf{M}\ddot{\mathbf{x}}(t) + \mathbf{C}\dot{\mathbf{x}}(t) + \mathbf{K}\mathbf{x}(t) + \mathbf{H}\mathbf{f}(t) = -\mathbf{G}\ddot{x}_g(t) \quad (1)$$

where the mass, damping and stiffness matrices are defined as

$$\mathbf{M} = \begin{bmatrix} \mathbf{M}_1 & \mathbf{0} \\ \mathbf{0} & \mathbf{M}_2 \end{bmatrix}, \quad \mathbf{C} = \begin{bmatrix} \mathbf{C}_1 & \mathbf{0} \\ \mathbf{0} & \mathbf{C}_2 \end{bmatrix}, \quad \mathbf{K} = \begin{bmatrix} \mathbf{K}_1 & \mathbf{0} \\ \mathbf{0} & \mathbf{K}_2 \end{bmatrix} \quad (2)$$

\mathbf{M}_j , \mathbf{C}_j and \mathbf{K}_j are the $N_j \times N_j$ dimensional mass, damping and stiffness matrices, respectively, for the j th structure ($j = 1, 2$). The loading influence vector \mathbf{G} for the ground acceleration $\ddot{x}_g(t)$ and the loading influence vector \mathbf{H} for the control force vector of coupling link $\mathbf{f}(t)$ in Eq. (1) are expressed as

$$\mathbf{G} = \begin{bmatrix} \mathbf{M}_1 \mathbf{1} \\ \mathbf{M}_2 \mathbf{1} \end{bmatrix}, \quad \mathbf{H} = \begin{bmatrix} \mathbf{H}_1 \\ -\mathbf{H}_2 \end{bmatrix}, \quad \mathbf{H}_1 = \begin{bmatrix} \mathbf{H}_2 \\ \mathbf{0} \end{bmatrix}, \quad \mathbf{1} = [1 \ 1 \ \dots \ 1]^T \quad (3)$$

where the matrices \mathbf{H}_1 with dimension $N_1 \times N$ and \mathbf{H}_2 with dimension $N_2 \times N$ indicate the location of control force $\mathbf{f}(t)$ to be applied.

2.2 Modeling of friction damper

By choosing passive friction dampers as joint devices between two buildings, the N -dimensional friction (control) force vector $\mathbf{f}(t) = [f_1(t) \ f_2(t) \ \dots \ f_N(t)]^T$ will be determined in accordance with the dampers' status of sticking and slipping. Coulomb law, the simplest and common model, is adopted for motion simulation of friction dampers. It presumes that the frictional force is independent of velocity and the kinetic coefficient μ_k is the only proportional constant considered in the mathematical relation between frictional force and normal force. The mathematical expression for friction force can be given by

$$f_i(t) = \begin{cases} k_{di}[x_i^{rel}(t) - e_i(t)] & \text{if } \bar{f}_i(t) \leq f_{di} \quad (\text{sticking}) \\ f_{di} \text{sgn}[\dot{x}_i^{rel}(t)] & \text{if } \bar{f}_i(t) > f_{di} \quad (\text{slipping}) \end{cases} \quad (4)$$

$$\bar{f}_i(t) = k_{di}[x_i^{rel}(t) - e_i(t)], \quad \text{sgn}[\dot{x}_i^{rel}(t)] = \begin{cases} 1 & \text{if } \dot{x}_i^{rel}(t) > 0 \\ -1 & \text{if } \dot{x}_i^{rel}(t) < 0 \end{cases} \quad (5)$$

in which the designed frictional slip force f_{di} (see Fig. 1) of the i th damper is grouped in the design frictional force vector $\mathbf{f}_d = [f_{d1} \ f_{d2} \ \dots \ f_{dN}]^T$; the i th damper elastic stiffness is denoted by k_{di} which is the i th element in a $N \times N$ diagonal stiffness matrix $\mathbf{K}_d = \text{diag}[k_{d1}, k_{d2}, \dots, k_{dN}]$; $x_i^{rel}(t)$ and $\dot{x}_i^{rel}(t)$ denote, respectively, the relative displacement and velocity between the adjacent buildings at the same floor where the i th damper is connected; $e_i(t)$ represents the slip deformation of the i th damper, and it is obtained through iterations from the following expression when the i th damper is in slipping status.

$$e_i = \bar{e}_i + \left| x_i^{rel} - \bar{e}_i \right| - \frac{|f_i|}{k_{di}} \text{sgn}[\dot{x}_i^{rel}] \quad (6)$$

where \bar{e}_i is the previous cumulated slip deformation of the i th damper. The coupled building system with passive friction damper as described above can be degraded to uncoupled case when choosing $k_{di} = f_{di} = 0$ and to rigid-coupled case when choosing $k_{di} \gg k_{i,j}$ as well as $f_{di} \gg W_{i,j}$, where $k_{i,j}$, and $W_{i,j}$ are the i th floor stiffness and floor weight of the j th building, respectively.

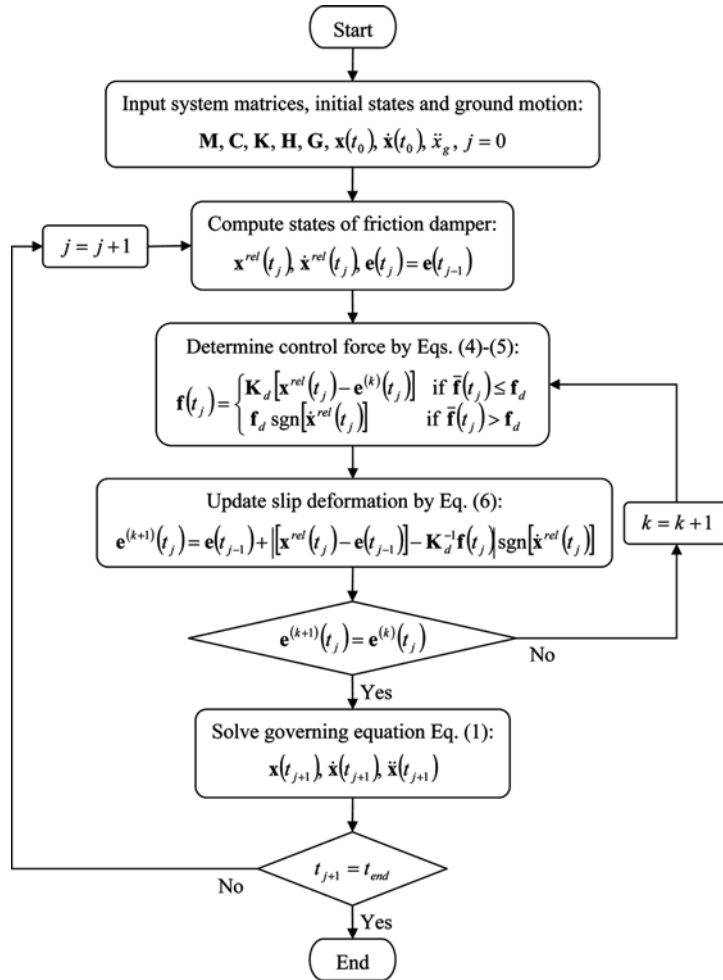


Fig. 2 Flowchart of numerical simulation for coupled building system

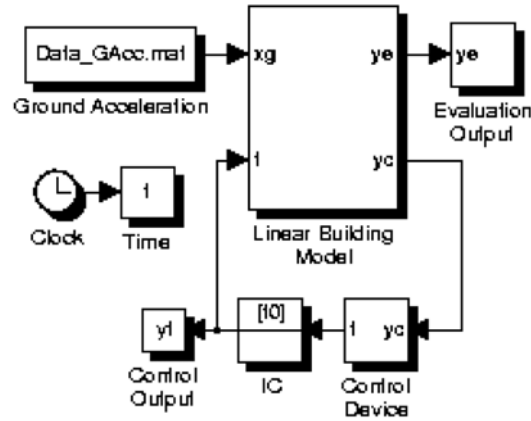


Fig. 3 Simulink block diagram for coupled building system

2.3 Numerical simulation

A flowchart regarding the numerical simulation of seismic vibration of the coupled building system with joint friction dampers is depicted in Fig. 2 for expression clarity. Attention should be paid to the determination of the i th damper's friction force $f_i(t)$, for which slip deformation is one of the dependent variables but the current slip deformation cannot be calculated simultaneously before the state of damper (i.e., slipping or sticking) is known. This blockage in calculation can be removed by taking the previous time step $e(t_{j-1})$ as a trial guess to proceed the determination of pseudo-friction force $\bar{f}(t_j)$, and iterations are then implemented to recalculate the actual friction force $f(t_j)$ and the slip deformation $e(t_j)$ at time t_j accordingly. By knowing the system states $\mathbf{x}(t_j)$ and $\dot{\mathbf{x}}(t_j)$, as well as the friction force $f(t_j)$ at time t_j , the seismic responses at time t_{j+1} can be computed by solving the governing equation. In this regard, the MATLAB software is used as the essential tool to complete the aforementioned task. Simulink block diagram for solving the nonlinear equation of motion of the coupled building system is schematically shown in Fig. 3. Ground acceleration is input to the linear building model and the control force from the friction dampers (control devices) is also accordingly determined based on the output responses including the relative displacement and velocity between the adjacent buildings as denoted by variable y_c in the block diagram. In addition, an initial condition block IC is used to solve the problem associated with the algebraic loop in the simulation. Time histories related to friction force and interested structural responses for control performance evaluation are recorded to workspace in variable y_j and y_e , respectively. The simulation solver with the Runge-Kutta method of fourth order at time interval of 0.01 sec is selected.

3. Dynamic implication of rigid-coupled buildings

In current practice, multi-story main buildings are often rigidly connected to a podium structure. The dynamic implications of the rigid-coupled building system are thus investigated against uncoupled buildings. A reformulated modal analysis method proposed by Chopra (1996) is embraced, whereby physical characteristics of dynamic responses can be specifically highlighted in

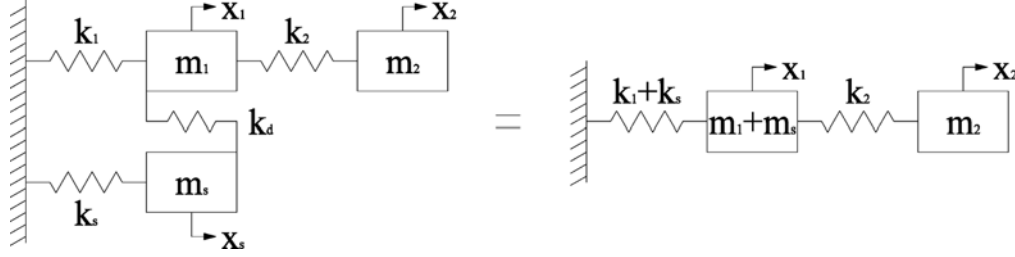


Fig. 4 A schematic diagram of equivalent 2-DOF coupled system

terms of modal responses in the exclusion of dynamic influence from ground motions. For completeness, changes in natural frequencies of uncoupled buildings as a result of rigid connection are first examined by considering an equivalent two-degree-of-freedom (2-DOF) rigid-coupled building system.

3.1 Changes in natural frequencies of rigid-coupled buildings

3.1.1 Basic characteristic

Consider a 3-DOF coupled system (see Fig. 4) which can be reduced to an equivalent 2-DOF coupled system in the case of rigid connection (i.e., $k_d \rightarrow \infty$, where k_d is the stiffness of coupling link). Assume that $m_1 = m_2 = m$, $k_1 = k_2 = k$, $m_s = \alpha m$ and $k_s = \beta k$, where α and β are any positive real number for frequency altering of the 1-DOF system. The system matrices and natural frequencies of the 2-DOF system can be expressed as

$$\mathbf{M} = \begin{bmatrix} (\alpha + 1)m & 0 \\ 0 & m \end{bmatrix}, \quad \mathbf{K} = \begin{bmatrix} (\beta + 2)k & -k \\ -k & k \end{bmatrix} \quad (7)$$

$$\omega_{1,2}^2 = \frac{1}{2m} k \left[\left(\frac{\beta + 2}{\alpha + 1} + 1 \right) \mp \sqrt{\left(\frac{\beta + 2}{\alpha + 1} + 1 \right)^2 - 4 \left(\frac{\beta + 1}{\alpha + 1} \right)} \right] \quad (8)$$

It can be examined that there are five cases defining the frequencies of rigid-coupled structures, which depend on the frequency of 1-DOF system by selecting appropriate value of α and β , (i) $\omega_{1,c}^2 < \omega_{1,u}^2$ and $\omega_{2,c}^2 < \omega_{2,u}^2$ if $k_s/m_s < \omega_{1,u}^2$; (ii) $\omega_{1,c}^2 > \omega_{1,u}^2$ and $\omega_{2,c}^2 > \omega_{2,u}^2$ if $k_s/m_s > \omega_{2,u}^2$; (iii) $\omega_{1,c}^2 > \omega_{1,u}^2$ and $\omega_{2,c}^2 < \omega_{2,u}^2$ if $\omega_{1,u}^2 < k_s/m_s < \omega_{2,u}^2$; (iv) $\omega_{1,c}^2 = \omega_{1,u}^2$ and $\omega_{2,c}^2 < \omega_{2,u}^2$ if $k_s/m_s = \omega_{1,u}^2$; and (v) $\omega_{1,c}^2 > \omega_{1,u}^2$ and $\omega_{2,c}^2 = \omega_{2,u}^2$ if $k_s/m_s = \omega_{2,u}^2$, where $\omega_{i,u}$ and $\omega_{i,c}$ denote the i th modal frequency of the uncoupled and coupled 2-DOF system, respectively. The cases (iv) and (v) are two special cases, which correspond to the case of frequencies coinciding between two uncoupled systems.

3.1.2 Numerical example

For the sake of numerical study, 20- (building 1) and 3-story (building 2) buildings are taken as basic building examples of the coupled building system, and they are also taken as basic coupled building system for the later dynamic response analysis. All floor masses of buildings 1 and 2 are 5.5×10^5 kg and 1.0×10^6 kg, respectively, and the corresponding uniform shear stiffness of buildings are 9.25×10^8 N/m and 8.65×10^8 N/m. 1% damping ratios for the first two modes are

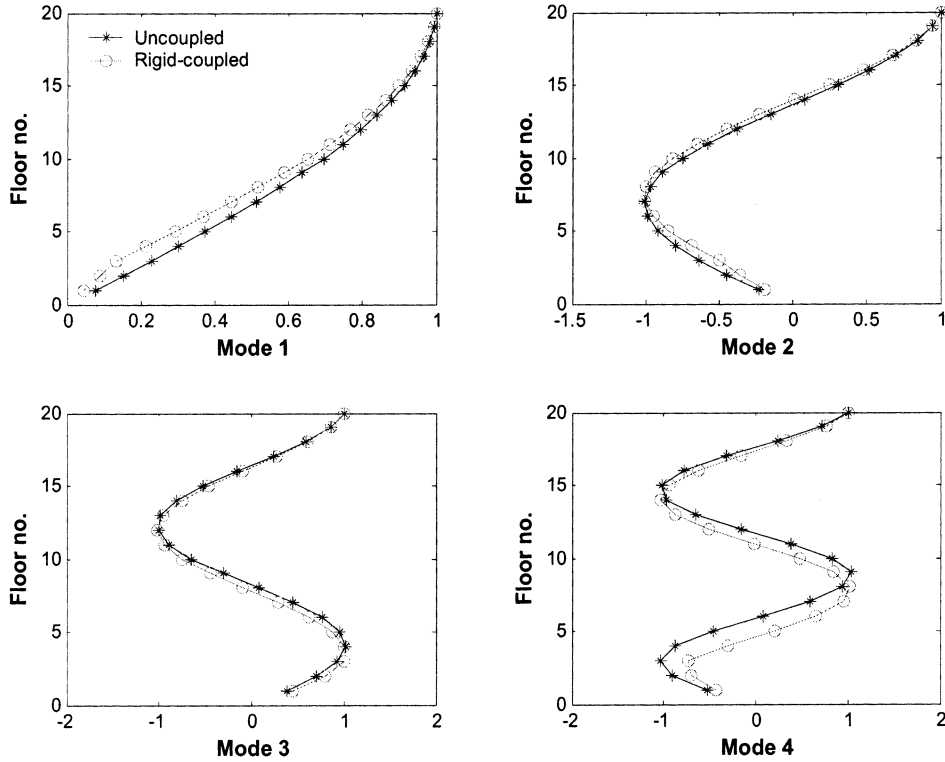


Fig. 5 Mode shapes for the 20- and 3-story coupled building system

selected for both buildings. By considering the first four natural frequencies of the uncoupled 20-story building, they are 0.50, 1.50, 2.49 and 3.46 Hz, respectively, and frequencies are accordingly 2.08, 5.84 and 8.44 Hz for the first three modes of the uncoupled 3-story building. The associated mode shapes of building 1 in both configurations are also illustrated in Fig. 5. It is observed that the fundamental frequency of 3-story building is ranked between the 2nd and 3rd modal frequencies of the 20-story building, and the first two natural frequencies of the 20-story building will be expected to increase when it is rigidly coupled with the 3-story building according to the above observation. The first four natural frequencies of the coupled building are 0.54, 1.56, 2.40 and 3.19 Hz, and these changes are consistent with the above findings. One should also notice that only slight changes in natural frequencies are observed due to the rigid-coupling, and the absolute percentage changes are 7.3, 4.2, 3.4 and 7.7%, respectively.

3.2 Effect of rigid connection on dynamic responses

3.2.1 Formulation of modal responses

To proceed the formation of responses with modal analysis method, it is first necessary to rewrite Eq. (1) into the form of

$$\mathbf{M}\ddot{\mathbf{x}}(t) + \mathbf{C}\dot{\mathbf{x}}(t) + \bar{\mathbf{K}}\mathbf{x}(t) = -\mathbf{G}\ddot{\mathbf{x}}_g(t) \quad (9)$$

in which $\bar{\mathbf{K}} = \mathbf{K} + \bar{\mathbf{K}}_d$; $\bar{\mathbf{K}}_d$ is the stiffness matrix of coupling links given by

$$\bar{\mathbf{K}}_d = \begin{bmatrix} \mathbf{K}_d & \mathbf{0} & -\mathbf{K}_d \\ \mathbf{0} & \mathbf{0} & \mathbf{0} \\ -\mathbf{K}_d & \mathbf{0} & \mathbf{K}_d \end{bmatrix} \quad (10)$$

Eq. (9) is firstly transformed to an uncoupled equation of SDOF system which is written as

$$\ddot{D}_n(t) + 2\zeta_n\omega_n\dot{D}_n(t) + \omega_n^2D_n(t) = -\ddot{x}_g(t) \quad (11)$$

where ω_n , ϕ_n and ζ_n are the natural frequency, mode shape and damping ratio for the n th mode of the original MDOF system; the response $D_n(t)$ is in fact related to the modal coordinate $q_n(t)$ and the modal participation factor Γ_n in the form of

$$q_n(t) = \Gamma_n D_n(t) \quad (12)$$

$$\Gamma_n = \frac{L_n}{M_n}, \quad L_n = \phi_n^T \mathbf{M} \mathbf{1}, \quad M_n = \phi_n^T \mathbf{M} \phi_n \quad (13)$$

Based on the above equations and equivalent static force concept suggested by Chopra (1996), the total response quantity $\mathbf{r}(t)$ can be expressed as

$$\mathbf{r}(t) = \sum_{n=1}^N \mathbf{r}_n(t), \quad \mathbf{r}_n(t) = \mathbf{r}_n^{coef} A_n(t), \quad A_n(t) = \omega_n^2 D_n(t) \quad (14)$$

where the n th modal response coefficient \mathbf{r}_n^{coef} of the n th modal response $\mathbf{r}_n(t)$ can be determined by static analysis of the structure under equivalent static force. The n th modal response coefficient $r_{i,n}^{coef}$ of the i th floor for the response of relative displacement $x_{i,n}$ with respect to ground, and story drift $\Delta_{i,n}$ at i th story are respectively given by

$$x_{i,n}^{coef} = \left(\frac{\Gamma_n}{\omega_n} \right) \phi_{i,n}, \quad \Delta_{i,n}^{coef} = \left(\frac{\Gamma_n}{\omega_n} \right) (\phi_{i,n} - \phi_{i-1,n}) \quad (15)$$

The floor acceleration can also be estimated by

$$\ddot{\mathbf{x}}_n(t) = -\ddot{\mathbf{x}}_n^{coef} A_n(t), \quad \ddot{x}_{i,n}^{coef} = \Gamma_n \phi_{i,n} \quad (16)$$

3.2.2 Interpretation of modal static responses

As above noted the total seismic responses can be expressed in terms of modal responses that are given by the product of time-invariant part \mathbf{r}_n^{coef} and dynamic part $A_n(t)$. The dynamic part is clearly dependent on the ground excitation and the natural frequencies of the system, whereas the time-invariant part is unaffected by the characteristic of ground excitation and is only responsive to the dynamic properties of the system alone. Taking the advantage of this feature, the coupling effect on various responses of the main building in terms of modal responses coefficient is studied. The coefficients of modal response quantities being taken into consideration are top floor displacement $x_{20,n}^{coef}$, 4th floor interstory drift $\Delta_{4,n}^{coef}$, and top floor acceleration $\ddot{x}_{20,n}^{coef}$. The top floor responses for displacement and acceleration are considered since obtained experimental results suggested that the largest magnitude always appeared at the top floor. Interstory drift at the 4th floor is, in contrast,

Table 1 Modal time invariant responses of uncoupled and rigid-coupled buildings

Responses	Mode			
	1	2	3	4
(a) 10-story building				
$x_{20,n}^{coef}$	0.045 (0.0385)	-0.0016 (-0.0031)	0.0003 (0.0006)	-0.0001 (-0.0002)
$\Delta_{4,n}^{coef}$	0.0059 (0.0063)	-0.0000 (-0.0003)	-0.0002 (-0.0004)	-0.0001 (-0.0001)
$\ddot{x}_{20,n}^{coef}$	1.2673 (1.4499)	-0.4068 (-0.6794)	0.2259 (0.3222)	-0.1429 (-0.1950)
(b) 20-story building				
$x_{20,n}^{coef}$	0.1288 (0.1165)	-0.0047 (-0.0061)	0.0010 (0.0020)	-0.0004 (-0.0007)
$\Delta_{4,n}^{coef}$	0.0095 (0.0094)	0.0008 (0.0012)	0.0001 (0.0001)	0.0000 (-0.0003)
$\ddot{x}_{20,n}^{coef}$	1.2717 (1.3236)	-0.4198 (-0.5851)	0.2469 (0.4537)	-0.1712 (-0.2874)
(a) 30-story building				
$x_{20,n}^{coef}$	0.2385 (0.2230)	-0.0088 (-0.0097)	0.0019 (0.0029)	-0.0007 (-0.0014)
$\Delta_{4,n}^{coef}$	0.0121 (0.1191)	0.0012 (0.0014)	0.0003 (0.0005)	0.0000 (0.0000)
$\ddot{x}_{20,n}^{coef}$	1.2725 (1.2970)	-0.4223 (-0.5005)	0.2511 (0.3885)	-0.1770 (-0.3353)

Note: Value in parenthesis represents response in rigid-coupled case

concerned because significant changes of the response at this location were detected from the test results when both structures were rigidly coupled.

The results of three modal responses for the first four modes of 20-story building in the cases of uncoupling and rigid-coupling are presented in Table 1. For each response quantity of either uncoupled or coupled building, its first modal response coefficient is the largest one among the four modal response coefficients. The absolute values of modal responses coefficient, in general, decrease monotonically for higher modes. Hence, in view of time-invariant part of the modal responses, it can be concluded that there is an inherent significance shared by the fundamental mode in the seismic vibration for the concerned building. To illustrate the relative contribution of higher mode with respect to the fundamental mode, the ratios of $|r_{i,n}^{coef}/r_{i,1}^{coef}|$ for the three responses are defined and those ratios regarding the second mode are selected for discussion in the following. The evaluated ratios for the uncoupled 20-story building are 0.04, 0.08 and 0.33, respectively, for the modal response coefficients of x_{20}^{coef} , Δ_{4}^{coef} , and \ddot{x}_{20}^{coef} . Dominancy of the first mode in response coefficient is highly noticeable for top-floor displacement. The ratios are accordingly increased to 0.05, 0.13, and 0.44 for the 20-story building being rigidly linked with the 3-story building. This result suggests that increasing proportion of higher modes in the total responses, particularly for the interstory drift and acceleration, will be resulted from rigid coupling. Nevertheless, the top-floor displacement is the least influenced response under the effect of rigid coupling, and total displacement response will be still exhibited as first-mode dominated for rigid-coupled building. To confirm these findings, 10- and 30-story buildings are additionally considered and the results are also summarized in Table 1, and similar conclusion can be drawn. For instance, the ratio of $|r_{i,n}^{coef}/r_{i,1}^{coef}|$ in regard to the 2nd acceleration modal response is increased from 0.32 (0.33) to 0.47 (0.39) for 10-story (30-story) building. It is worthwhile to note that the first acceleration modal coefficient is also increased when the two buildings are rigidly coupled.

3.2.3 Design implications

One great advantage of the modal analysis is its compatibility with seismic design by referring to a design spectrum, and total peak responses can be determined by employing modal combination method of square-root-of-sum-of-squares (SRSS) or complete quadratic combination (CQC). It is known that design spectrum consists of smooth curves or a series of straight lines with one curve for particular level of damping that represents the average characteristics of various ground motions. Typical example of pseudo-acceleration design spectrum is shown in Fig. 6 (Chopra 1996). By recognizing this property of design spectrum and recalling that the differences of the natural frequencies between uncoupled and rigid-coupled buildings are negligible, the corresponding values of pseudo-acceleration for the two kinds of buildings are thus not expected to differ largely. Therefore, the response coefficient r_n^{coef} of all modal responses seem acting as key indicators to reveal the design effectiveness between uncoupled and rigid-coupled buildings. Based upon this fact, it is apparently that the rigid-coupled building system will normally be associated with larger drifts and accelerations than the uncoupled building system counterparts. Furthermore, larger proportion of higher mode responses will be shared in the total responses of rigid-coupled buildings because of increased modal coefficient and higher spectrum values for the higher modes (see Table 1 and Fig. 6). To alleviate seismic vibrations of the rigid-coupled building system, the coupling control strategy using joint dampers probably offers an alternative method to avoid amplifying responses in rigid connection case and pounding problem in uncoupled case. The degree of coupling can be manipulated and the structural vibration energy can be simultaneously dissipated with the aid of joint dampers.

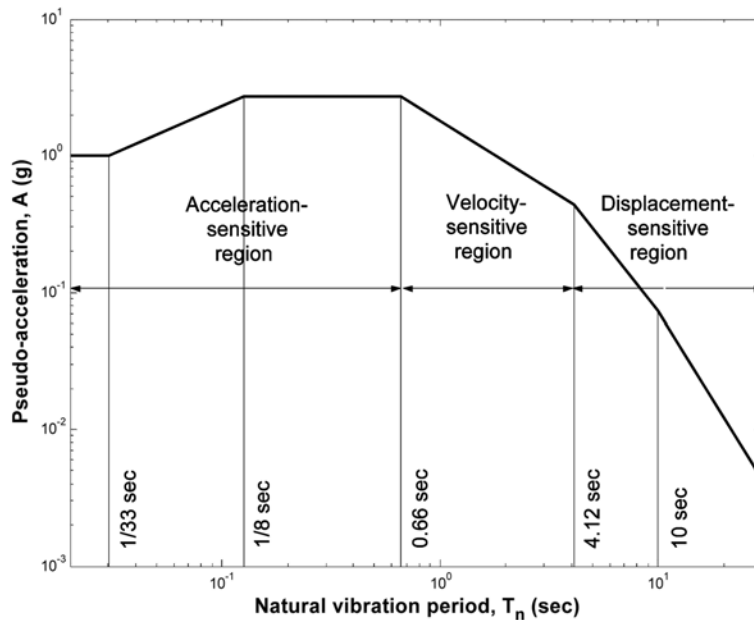


Fig. 6 Elastic pseudo-acceleration design spectrum (84.1th percentile) for ground motions with $\ddot{x}_{go} = 1g$, $\dot{x}_{go} = 48$ in./sec, and $x_{go} = 36$ in.; $\zeta = 0.5\%$ (Chopra 1996)

4. Buildings interconnected with friction dampers

To fully understand the interaction control scheme implemented in a coupled building system with passive friction dampers, parametric studies are started with an investigation on selection of optimal design friction slip force for the coupled building system employed with a single friction damper. The objective is to evaluate the relationship between variation of optimal friction force and change of internal as well as external factors associated with the coupled building system. Internal factors refer to floor mass and story number difference between two buildings, and input ground motion is regarded as an external factor. Effects of those internal and external factors on control performance of damper-coupled building scheme are subsequently discussed. Control effectiveness of building seismic responses with multiple friction dampers is also investigated and discussed in this section.

Four performance indices, of which responses include displacement, interstory drift, acceleration and base shear, are selected for quantitative evaluation of the ability in alleviating seismic vibration by friction dampers in comparison to the uncoupled buildings. The indices are defined as

$$J_1 = \frac{\max_i [x_{i,j}^{rms}]}{x_j^{rms}}, \quad J_2 = \frac{\max_i [\Delta_{i,j}^{rms}]}{\Delta_j^{rms}}, \quad J_3 = \frac{\max_i [\ddot{x}_{i,j}^{rms}]}{\ddot{x}_j^{rms}}, \quad J_4 = \frac{\max_i [V_{b,j}^{rms}]}{V_{b,j}^{rms}} \quad (17)$$

where $x_{i,j}^{rms}$, $\Delta_{i,j}^{rms}$, $\ddot{x}_{i,j}^{rms}$ and $V_{b,j}^{rms}$ are the i th floor displacement, interstory drift, absolute acceleration and base shear rms responses, respectively, of the j th building with joint dampers ($j = 1, 2$); the corresponding responses in the maximum rms value of the j th uncoupled building are denoted by x_j^{rms} , Δ_j^{rms} , \ddot{x}_j^{rms} and $V_{b,j}^{rms}$. These four performance indices are taken to be the determination criteria of design friction force because rms value will take full time series into consideration which is a better indicator of energy dissipation capability of friction damper. Earthquakes employed for input ground motions in the parametric studies are El Centro NS (1940, PGA = 3.417 m/s²), Hachinohe NS (1968, PGA = 2.250 m/s²), Kobe NS (1995, PGA = 8.178 m/s²) and Northridge NS (1994, PGA = 8.267 m/s²).

4.1 Design range of optimal friction force

Determination of the optimal parameters of single damper to minimize various structural responses is based on two dimensionless parameters. Parameters are associated with the design friction force and stiffness of the damper interconnected the buildings 1 and 2, and they are given by

$$\text{Slip load ratio } \alpha = \frac{f_{di}}{W_{ave,1}}, \quad \text{Damper stiffness ratio } \beta = \frac{k_{di}}{k_{ave,1}} \quad (18)$$

where $W_{ave,1}$ and $k_{ave,1}$ are the average floor weight and average floor stiffness of building 1, respectively. Determining the design friction force f_{di} in terms of slip load ratio α can develop a clear relationship with the floor weight of building and also provide an intuitive insight of force magnitude. The slip load ratio α (i.e., design friction force) attains its optimum value when the performance indices are minimized. It is evaluated that the response reduction is insensitive to the stiffness of the coupling friction damper when the damper stiffness ratio β beyond 0.5, and this characteristic is regardless of the input earthquake records. The typical results are demonstrated in Fig. 7. Therefore, all parametric studies below are performed with parameter of damper stiffness ratio β being fixed to 1.0.

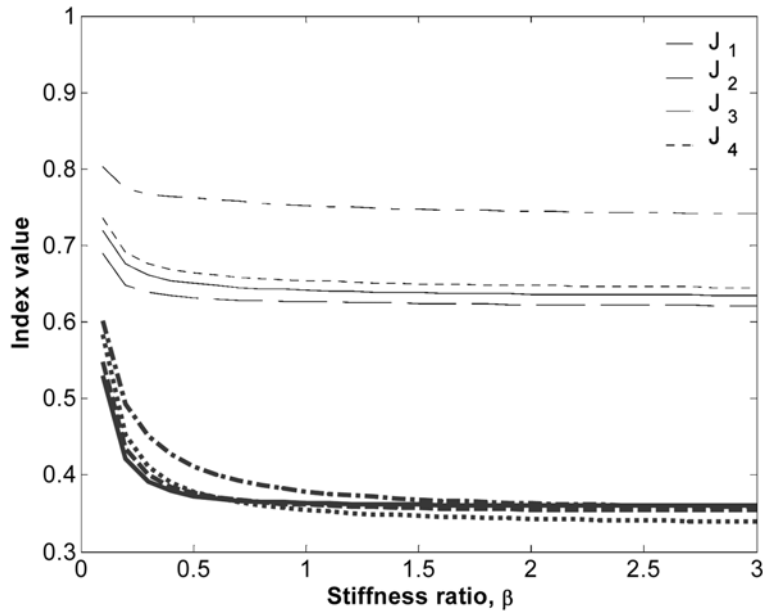
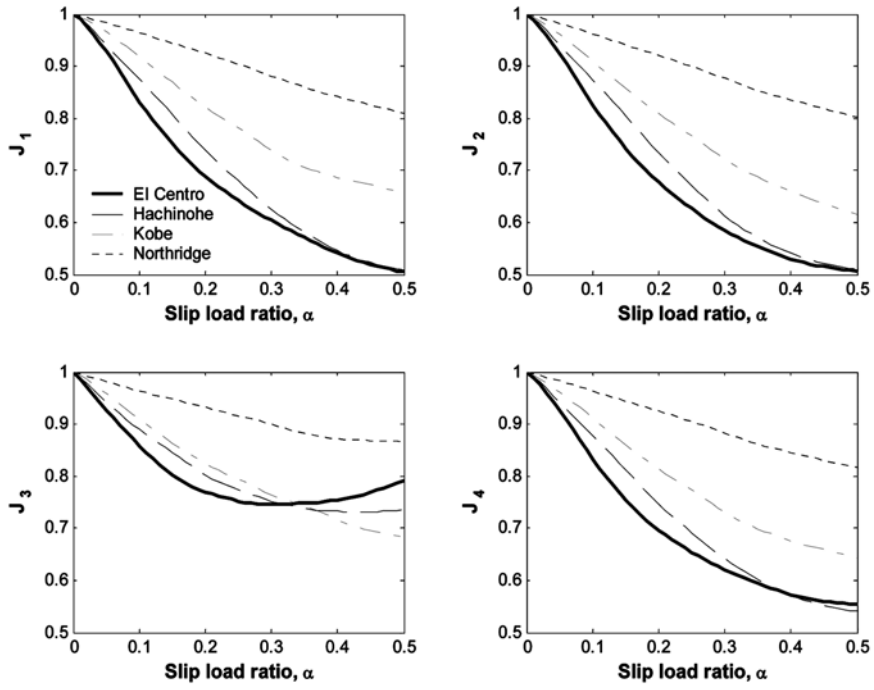


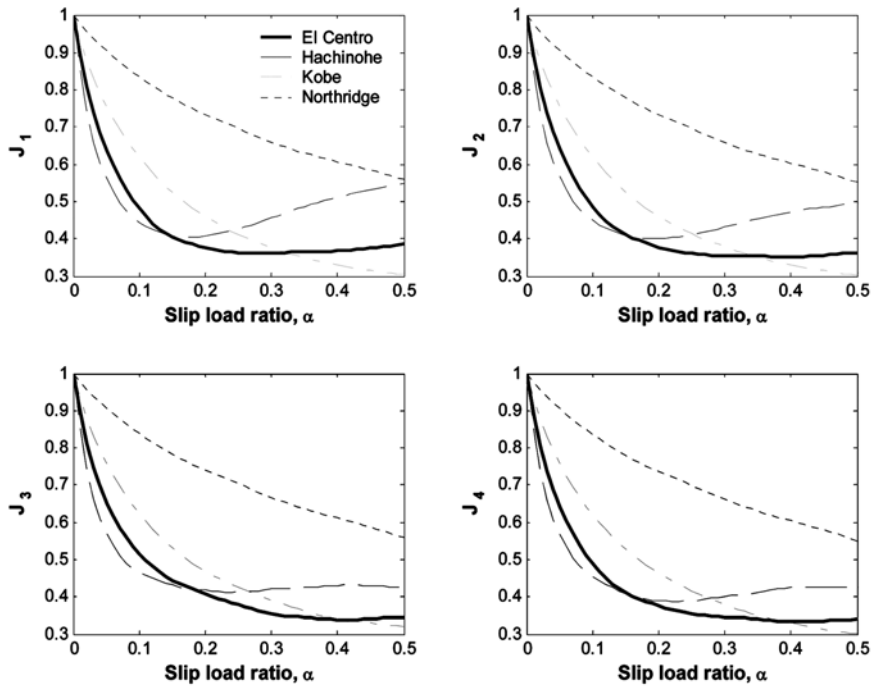
Fig. 7 Variation of performance indices for building 1 (light line) and building 2 (heavy line) with damper stiffness ratio β with slip load ratio $\alpha = 0.25$ under El-Centro earthquake

4.1.1 Effect of earthquakes

The influence of input ground motions upon the design friction force is first studied. Figs. 8(a) and (b) show the curves of performance indices (J_1 to J_4) against the slip load ratio α varying within a range of $[0, 0.5]$, in which $\alpha = 0$ corresponds to the main and podium structures being uncoupled. The first observation is that variation trend, disregarding the decreasing rate, of the indices for building 1 is consistent for all earthquakes. The optimal point is not yet attained within the full concerned range of α for the indices related to responses of displacement, interstory drift and base shear. Unlike other responses, an optimal point is indicated for acceleration response (J_3) subjected to the El Centro and Hachinohe earthquakes, and the corresponding slip load ratio $\alpha \cong 0.25$ to 0.35 . All points mentioned above suggest that acceleration response of building 1 is better controlled at a lower level of design friction force, while other responses are not optimally reduced at that level of friction force. In other words, designing a higher level of design friction force to achieve the greatest reduction of displacement, interstory drift or base shear will lead to smaller reduction on acceleration response. A balance consideration of reduction among all responses is the key point on the decision of design friction force. On the other side, there exists an optimal slip load ratio ($\alpha \cong 0.25$) for all indices of building 2 subjected to earthquakes of El Centro and Hachinohe, whereas no optimal slip load ratio can be located for responses induced by the Kobe and Northridge earthquakes. Optimal slip load ratio can be identified at lower value for building 2 rather than building 1 is likely because damper is installed at the top floor, which is certainly the most effective location to reduce vibration of any responses, of building 2. In consideration of earthquake effect on slip load ratio, it is known that the Kobe and Northridge earthquakes possess much larger peak ground acceleration (PGA) than those of the El Centro and Hachinohe earthquakes, and the optimal slip load ratio α for both buildings thus appears at larger



(a) Building 1



(b) Building 2

Fig. 8 Comparison of performance indices under variation of slip load ratio for 4 ground motions

value. As a result, the slip load ratio α inside the range of 0.2-0.3 (i.e., 20%-30% of floor weight of the building 1) is suggested to use in the later study because it is practically reasonable and fair reduction is achieved among all responses of both buildings.

4.1.2 Effect of building configuration

Any significant variation of optimal slip load ratio upon the changes in floor mass and story number differences between two coupled buildings are investigated and the results are depicted in Figs. 9 and 10, respectively. It should be pointed out that all results presented below are studied under the El Centro earthquake only unless otherwise indicated. Only building 2 is liable to a floor mass change by multiplying a factor γ to the mass $m_{i,2}$ of every floor, and the stiffness of every floor of building 2 also proportionally increases or decreases by the same factor. Maintaining the ratio equal gains the advantage of keeping the natural frequencies of uncoupled building 2 unchanged and thus can independently study the effect of varying the floor mass of building 2 on the optimal slip load ratio α . Three sets of floor mass factor γ (0.5, 1.0 and 2.0) are considered. Fig. 9 shows that no considerable changes of response curves for building 1 are found. Unlike building 1, for building 2 the smaller the mass factor γ is, the lower will be the optimal slip load ratio α . Furthermore, the magnitudes of most performance indices remain quite steady beyond the optimal value of slip load ratio. These results imply that mass difference between two buildings is not a crucial factor in the design of friction force. For the parameter of story number difference, which is introduced as the story ratio λ , between two coupled buildings, by fixing the story number of building 2 to be three building 1 in 10-, 20-, and 30-story is studied. Although building 2 is coupled

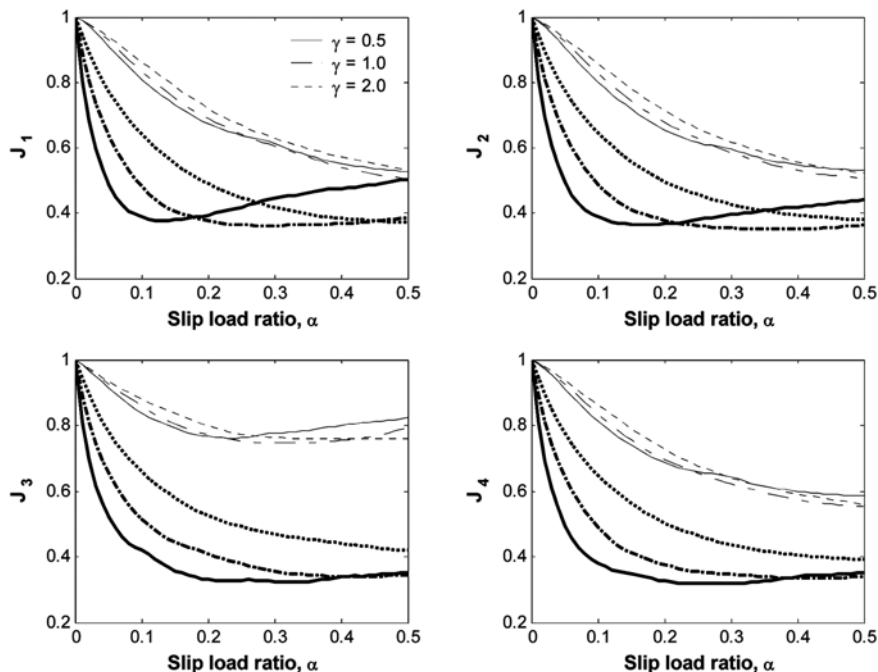


Fig. 9 Variation of optimal slip load ratio α for building 1 (light line) and building 2 (heavy line) with floor mass difference between two buildings

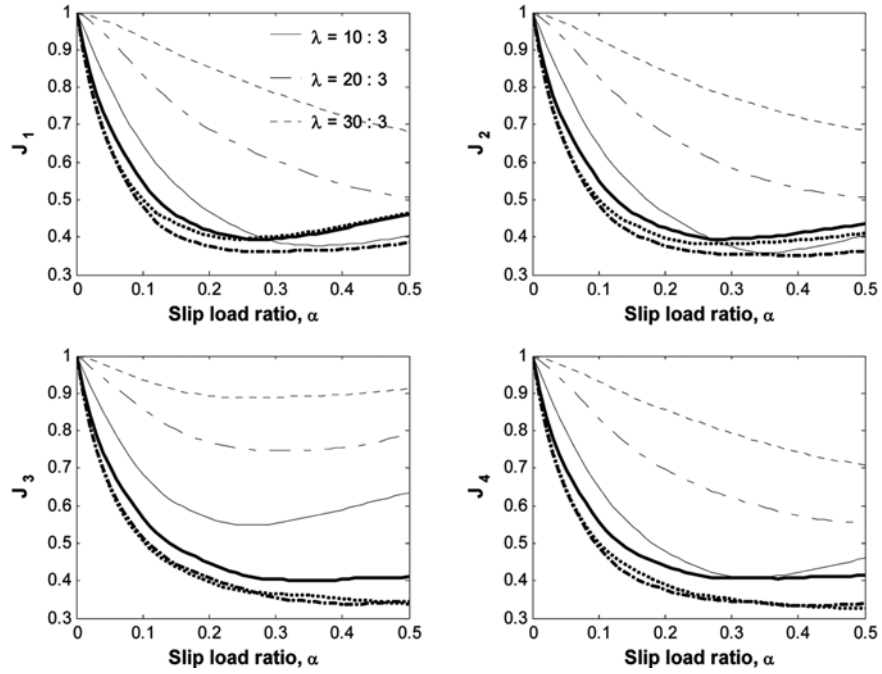


Fig. 10 Variation of optimal slip load ratio α for building 1 (light line) and building 2 (heavy line) with story number difference between two buildings

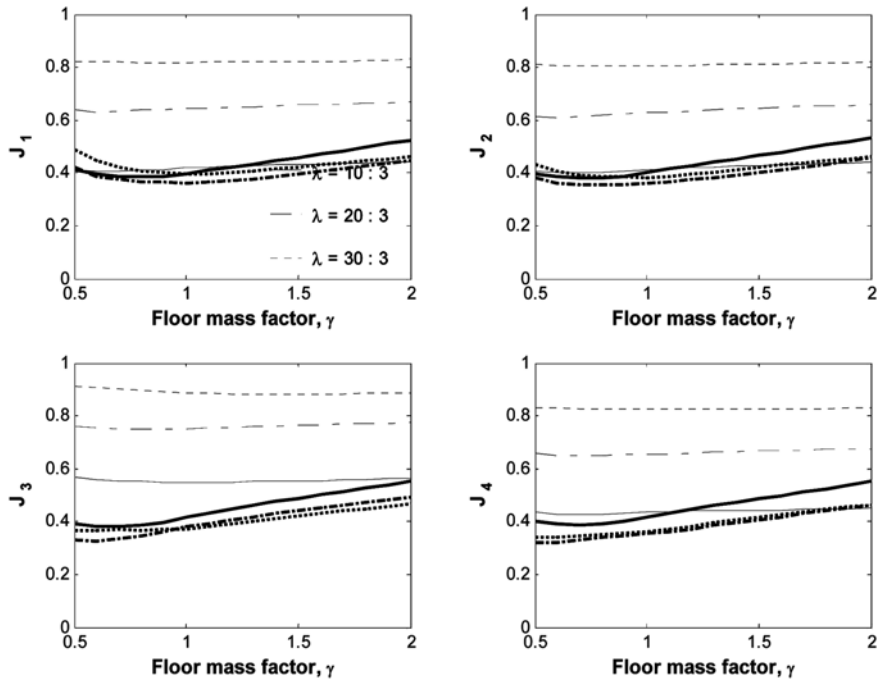


Fig. 11 Variation of performance indices for building 1 (light line) and building 2 (heavy line) with the change of floor mass and story number differences between two buildings

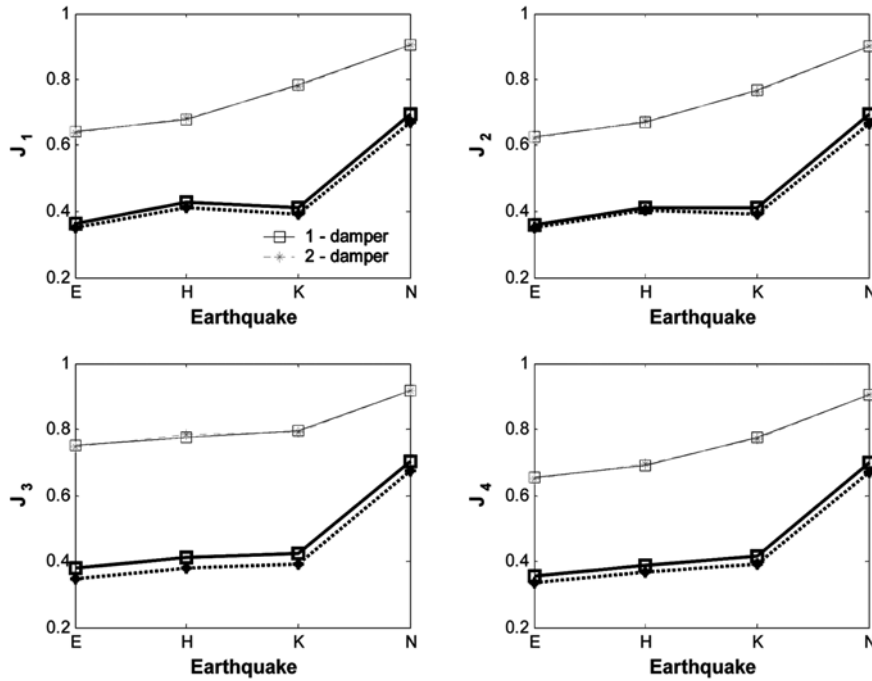


Fig. 12 Comparison of performance indices of building 1 (light line) and building 2 (heavy line) with 1- or 2-damper

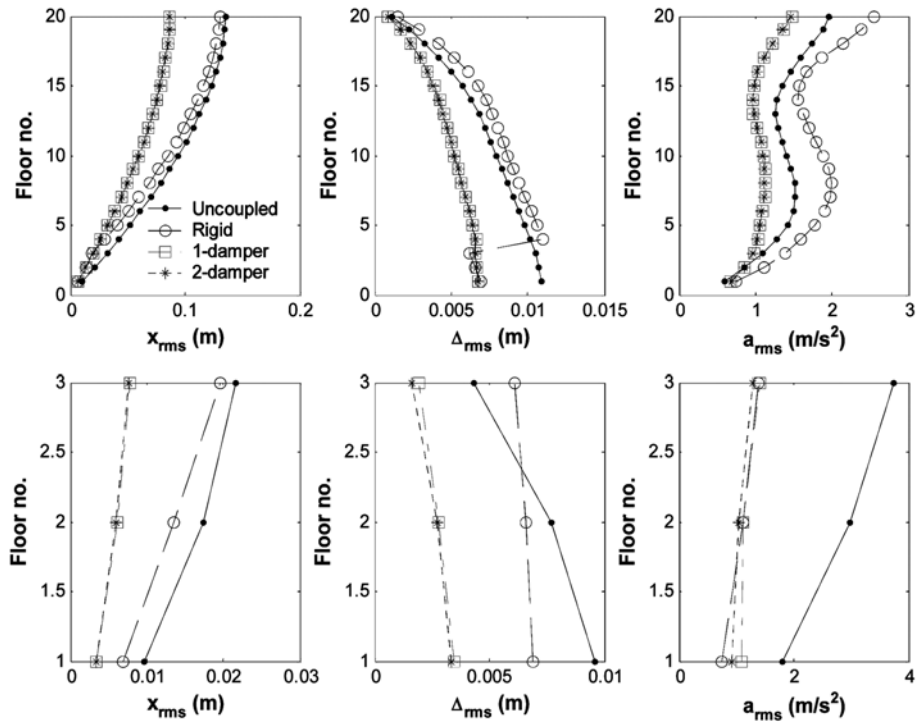


Fig. 13 Comparison of rms response profiles for coupled building system in various coupling configurations

to building 1 with different story number, there are nearly no changes for the curves of all performance indices of building 2 as shown in Fig. 10, and the optimal range of slip ratio α for building 2 is approximately kept at 0.2-0.3. In view of the optimal slip load ratio α of building 1, the results illustrate that friction damper can be designed at a relatively lower optimal friction force level for building 1 with less stories. This is also a reasonable phenomenon as the location of damper installed with respect to building 1 is more far from its top floor, which is believed to be the most favorable location in order to achieve better control of whole building, when its story number increases further. As a whole, designing the friction force at around 20%-30% of floor weight of building 1 (i.e., $\alpha = [0.2, 0.3]$) is seemed to be a quite practical and favorable control force level for both buildings.

4.2 Control efficacy of single passive friction damper

As discussed most of the maximum rms responses, of either building 1 or building 2, are best minimized approximately at slip load ratio $\alpha = [0.2, 0.3]$, design friction force is thus assigned with the slip load ratio $\alpha = 0.25$ for subsequent studies, and all control effectiveness comparisons below are based on this slip load ratio. Normalized vibration reductions of four maximum rms responses (J_1 to J_4) under the parameter variation of floor mass factor γ from 0.5 to 2.0, as well as the consideration of three different story ratio λ (30:3, 20:3, and 10:3) are illustrated in Fig. 11. It is clearly seen that reduction for all responses of building 1 is rather insensitive to the floor mass changes of building 2, but comparatively larger deviation of reduction is shown when the story ratio λ increases, i.e., the story number of building 1 increases. In contrast, response reduction of building 2 seems to be regardless of the changes in story number of building 1 because more or less 60% reduction is steadily maintained over the entire range of floor mass factor. In addition, no more than 10% decrease in reduction of all responses is demonstrated when its floor mass factor γ increases to 2.0, which is roughly equivalent to 3.5 times the floor mass of building 1.

4.3 Control efficacy of multiple passive friction dampers

Any potential benefit in using multiple dampers instead of single damper for coupled building control is the key issue being explored in this section. 2-damper assembly layout is considered for the case of multiple dampers, and each damper is installed at the second and the third floor, respectively. Slip load ratio $\alpha = 0.15$ is designed based on the optimization of performance indices J_1 , J_2 , J_3 , and J_4 . In addition, four earthquake records are used to provide more comprehensive comparison of control efficacy between configuration of 1-damper and 2-damper. Four performance indices related to the maximum rms responses for the coupled buildings with 1-damper and 2-damper assembly are compared in Fig. 12. The letters 'E', 'H', 'K', and 'N' under the x -axis of Fig. 12 denote the earthquakes of El Centro, Hachinohe, Kobe and Northridge, respectively. The results clearly illustrate that there are completely no significant differences in control performance for all responses of buildings installed with 1-damper or 2-damper over all earthquakes. However, it should be reminded that the design friction force of individual damper in 2-damper assembly is 15% floor weight of the building 1. It is important that this friction force is 60% smaller than that of damper in 1-damper assembly ($\alpha = 0.25$), suggesting smaller scale of damper can be used. In other words, engineers are allowed with plenty room of design feasibility on decision of adopting single-damper or multiple-damper layout. There is less need to concern about deterioration of

control effectiveness between two schemes, while the choice of damper scale would be the prime consideration. Response profiles under excitation of El Centro earthquake as shown in Fig. 13 further provide a better expression of control performance between 1-damper and 2-damper design schemes. It is worthy to emphasize again that interaction control of coupled buildings by friction dampers is a promising method to mitigate seismic vibration of both buildings. Rigidly coupling two buildings is the worst construction method in view of seismic design because this will lead to the responses of acceleration and interstory drift of building 1 to be greatly provoked (see Fig. 13). In view of top floor rms acceleration of the rigidly coupled 20-story building under El-Centro earthquake, installation of friction damper can reduce the rms acceleration from 2.57 to 1.50 m/s², which corresponds to 41% reduction. Therefore, the coupling control could be a desirable construction scheme to replace the rigid-coupling practice for such building system of which there are potential unfavorable vibrations.

4.4 Practical considerations of passive friction damper

The above numerical study has demonstrated that the use of passive friction dampers with single- or multiple-floor linkage to couple and control a building complex is effective for earthquake hazard mitigations. Its long-term application very much depends on the reliability of such devices. A change of design magnitude of friction force as a result of loss of preload and changes in coefficient of friction are of critical concern. A variety of passive friction dampers have been developed in large-scale and applied to real building structures. Typical examples include X-braced friction damper (Pall and Pall 1996), Simitomo friction damper (Aiken and Kelly 1990), energy dissipating restraint (Nims *et al.* 1993, slotted bolted connection energy dissipator (FitzGerald *et al.* 1989, Grigorian *et al.* 1993), and friction damper devices (Mualla and Belev 2002). From the latest large-scale test on a three-storey steel frame structure equipped with friction-damping devices for seismic mitigation (Liao *et al.* 2004), it has been noted that reliability of friction damper could be stably high given that the damper is designed properly with friction pad materials. Using other kinds of passive control devices such as yielding steel devices as alternative is also practically possible and reliable, whereas friction damper could be used to mitigate vibration at both serviceability and ultimate levels and could be repeatedly used at a relatively low maintenance cost.

5. Conclusions

The possibility of using passive friction dampers to link a podium structure to a main building to enhance seismic resistance of coupled building system has been explored analytically in this study. Rigid interconnection of both buildings is the most common design practice for coupled building system, and pin-point study is thus first conducted to explore its dynamic implication with the aid of modal analysis method. Results demonstrate that responses of interstory drift and acceleration of the rigidly coupled main building are subjected to enlargement, and thus highlight the potential benefit of the coupling control because of its dual function of energy dissipation and pounding avoidance. The control performance of passive friction damper in vibration reduction is then extensively studied. The parametric study takes account of the factors of ground motions variety, floor mass and story number differences between the coupled buildings. Practical design range of friction force that yields most of the structural responses in a minimum value is approximately

about 20-30% of the average floor weight of the main building. The effect of the above mentioned factors imposed on the optimal friction force range is generally slight, whereas ground motions are probably the more influential factor in the design of appropriate force level. Regarding control effectiveness, a stable control performance is usually achieved by the supplemental friction devices. With uncoupled 20- and 3-story buildings as comparison basis, there are normally over 35% reduction reached for the maximum rms response regarding displacement, interstory drift and base shear of the main building, and acceleration response is also reduced by 25% at most. Difference in story number (or height) between two buildings is a crucial factor that affects the level of response mitigation of the main building. Nevertheless, a highly stable and robust control performance is noted for the prodium structure, and there are around 40-60% reductions of maximum rms responses attained. The multiple-damper scheme is lastly examined and the same control capability is revealed by comparing with single-damper deployment but with smaller friction force.

Acknowledgements

The funding support to this research by The Hong Kong Polytechnic University through a postgraduate scholarship to the first author is gratefully acknowledged.

References

- Aiken, I.D. and Kelly, J.M. (1990), "Earthquake simulator testing and analytical studies of two energy-absorbing systems for multistory structures", Rep. No. UCB/EERC-90-03, University of California, Berkeley, California.
- Arnold, C. (1980), "Building configuration: Characteristics for seismic design", *Proc. Seventh World Conf. on Earthq. Engrg.*, **4**, 589-592, Istanbul, Turkey.
- Arnold, C. and Elsesser, E. (1980), "Building configuration: Problems and solutions", *Proc. Seventh World Conf. on Earthq. Engrg.*, **4**, 153-160, Istanbul, Turkey.
- Chopra, A.K. (1996), "Modal analysis of linear dynamic systems: Physical interpretation", *J. Struct. Eng.*, **120**(5), 517-527.
- Constantinou, M.C., Soong, T.T. and Dargush, G.F. (1998), *Passive Energy Dissipation Systems for Structural Design and Retrofit*. Monograph series, MCEER, Buffalo, N.Y..
- Constantinou, M.C., Tsopelas, P., Hammel, W. and Sigaher, A.N. (2001), "Toggle-brace-damper seismic energy dissipation systems", *J. Struct. Eng.*, **127**(2), 105-112.
- FitzGerald, T.F., Anagnos, T., Goodson, M. and Zsutty, T. (1989), "Slotted bolted connections in aseismic design for concentrically braced connections", *Earthquake Spectra*, **5**, 383-391.
- Gardis, P.G. *et al.* (1982), *The Central Greece Earthquakes of February-March 1981*. A Reconnaissance and Engineering Report, National Academy Press, Washington, D.C..
- Gluck, J. and Ribakov, Y. (2001), "High efficiency viscous damping system with amplifying braces for control of multistory structures subjected to earthquakes", *European Earthq. Eng.*, **2**, 3-27.
- Grigorian, C.E., Yang, T.S. and Popov, E.P. (1993), "Slotted bolted connection energy dissipators", *Earthquake Spectra*, **9**(3), 491-504.
- Gurley, K., Kareem, A., Bergman, L.A., Johnson, E.A. and Klein, R.E. (1994), "Coupling tall buildings for control of response to wind", *Structural Safety and Reliability*, **3**, 1553-1560, Balkema, Rotterdam.
- Hanson, R.D., Aiken, I.D., Nims, D.K., Richter, P.J. and Bachman, R.E. (1993), "State-of-the-art and state of the practice in seismic energy dissipation", *Proc. Seminar on Seismic Isolation, Passive Energy Dissipation and Active Control*, **2**, 449-472, Applied Technology Council.
- Kageyama, M., Yasui, Y., Suzuki, T. and Seto, K. (1999), "A study on optimum design of joint dampers connecting two towers: The case of connecting two same height towers at multiple points", *Proc. of the*

- Second World Conf. on Structural Control*, **2**, 1463-1472, Chichester.
- Kamagata, K., Miyajima, K. and Seto, K. (1996), "Optimal design of damping devices for vibration control of parallel structures", *Proc. Third Int. Conf. on Motion and Vibration Control*, **2**, 334-339, Chiba.
- Klein, R.E., Cusano, C. and Stukel, J. (1972), "Investigation of a method to stabilize wind induced oscillation in large structures", *ASME Winter Annual Meeting*, 72-WA/AUT-H, New York.
- Liao, W.L., Mualla, H.I. and Loh, C.H. (2004), "Shaking-table test of a friction-damped frame structure", *The Structural Design of Tall and Special Buildings*, **13**, 45-54.
- Mualla, H.I. and Belev, B. (2002), "Performance of steel frames with a new friction damper device under earthquake excitation", *Eng. Struct.*, **24**, 365-371.
- Ng, C.L. and Xu, Y.L. (2004), "Experimental study on seismic response mitigation of complex structure using passive friction damper", *2004 ANCER Annual Meeting: Networking of Young Earthquake Engineering Researchers and Professionals*, Hawaii.
- Nims, D.K., Richter, P.J. and Bachman, R.E. (1993), "The use of the energy dissipating restraint for seismic hazard mitigation", *Earthquake Spectra*, **9**(3), 467-489.
- Pall, A.S. and Pall, R. (1996), "Friction-dampers for seismic control of buildings-A Canadian experience", *Proc., 11th World Conf. on Earthquake Engineering*, Paper No. 497.
- Ribakov, Y. and Reinhorn, A.M. (2003), "Design of amplified structural damping using optimal considerations", *J. Struct. Eng.*, **129**(10), 1422-1427.
- Soong, T.T. and Dargush, G.F. (1997), *Passive Energy Dissipation Systems in Structural Engineering*, Wiley, Chichester, U.K..
- Sugino, S., Sakai, D., Kundu, S. and Seto, K. (1999), "Vibration control of parallel structures connected with passive devices designed by GA", *Proc. of the Second World Conf. on Structural Control*, **1**, 329-337, Chichester.
- Suzuki, Z. ed. (1971), *General Report on the Takachi-Oki earthquake of 1968*. Keigshu Publishing Co., Tokyo, Japan.
- Taylor, D.P. (2002), "Toggle brace dampers: A new concept for structural control", *Advanced Technology in Structural Engineering: Proc. 2000 Structures Congress and Exposition (CD-ROM)*, ASCE, Reston, Va, Section, Chap. 3.
- Westermo, B.D. (1989), "The dynamics of interstructural connection to prevent pounding", *Earthq. Eng. Struct. Dyn.*, **18**, 687-699.